Solar Energy Materials & Solar Cells 125 (2014) 78–86

Contents lists available at ScienceDirect

Solar Energy Materials & Solar Cells

journal homepage: www.elsevier.com/locate/solmat

Optimization of front-contact laser scribing for thin-film silicon solar modules

Bugra Turan [a,*], Stefan Haas [a], Michael Steger [b]

[a] IEK5 - Photovoltaik, Forschungszentrum Jülich GmbH, 52425 Jülich, Germany
[b] Fraunhofer ILT, Steinbachstraße. 15, 52074 Aachen, Germany

ARTICLE INFO

Article history:
Received 21 September 2013
Received in revised form
17 February 2014
Accepted 18 February 2014
Available online 15 March 2014

Keywords:
Laser ablation
Thin-film
Solar module
Front-contact
Dead area
Heat-affected zone

ABSTRACT

The minimization of area losses for the integrated series connection of thin-film silicon solar modules is investigated for the front-contact separation process (P1). Sputtered ZnO:Al and commercially available SnO_2:F front-contact TCO material on glass substrates were used for laser ablation processing. Problems and limits of width reduction were identified for processing wavelengths of 355 nm, 532 nm, and 1064 nm. Minimal scribe widths of 10 μm were achieved with sufficiently high process stability. Material modifications near the scribe edge and their impact on the cell performance were characterized. Electrical properties of the TCO material after P1 processing were investigated with conductive Atomic Force Microscopy. Surface morphology analysis with Scanning Electron Microscopy showed redeposition of ablated material in vicinity of the scribe. The influence on the solar cell current generation was evaluated qualitatively with Laser Beam Induced Current measurements. Both material systems were characterized with and without subsequent wet-chemical cleaning/etching treatment after laser processing. With treatment, solar cell deterioration near the scribe edge was greatly reduced implying that material modifications originate from debris surface redeposition rather than heat-affected zone formation.

1. Introduction

Thin-film photovoltaic technology offers many advantages compared to wafer-based crystalline silicon technology. Some of these are low weight, low material consumption, flexible modules, building integration (BIPV), and in the case of thin-film silicon, material abundance. Another significant benefit is the possibility to generate an integrated series connection monolithically on one substrate [1]. The interconnection is realized by a selective removal of the functional layers during the production process. After each deposition process, laser ablation and/or mechanical scribing is used to precisely remove the individual layers. However, the area required for the interconnection is no longer active for current generation. Fig. 1 shows a sketch of an interconnected thin-film cell stripe layer stack in superstrate topology. The series connection is realized by the three individual scribes P1, P2, and P3 [2]. The required width of P1–P3 with the margins in between is depicted by the dead area width w_d. The width of the remaining active section is defined by the active cell width w_a. The power losses of the interconnected thin-film module are defined by the dead area fraction f_d and the TCO loss fraction f_{TCO}. Fig. 2 shows a calculation of the relative module losses $f = f_d + f_{TCO}$ vs. the active cell width w_a with measured cell parameters of an a–Si : H/μc–Si : H tandem solar cell for several interconnection widths w_d in accordance with a model proposed by Gupta et al. [3]. With decreasing dead area width w_d from 300 μm to 50 μm, the overall loss fraction sum f decreases from 5% down to about 2%. The minimization of the interconnection width w_d is therefore one important approach to increase the overall module efficiency.

Previous works about TCO laser processing are mainly about front-contact material ablation behavior and scribe quality. Some of these showed the influence of pulse duration and illumination geometry with different processing wavelengths for different TCO material systems [4,5]. Ku et al. compared different approaches of ablation threshold determination for film-side processing of aluminum-doped zinc oxide (ZnO:Al) and electrical insulation between neighboring TCO stripes after deposition of highly conductive μc–Si : H p-doped layers [6]. Recent works from Canteli et al. showed changes in the TCO microstructure by Raman spectroscopy near the scribe edge which can originate from heat-affected zone formation [7,8]. Furthermore, some analysis of the electrical properties of molybdenum (CIGS) near the scribe edge has been done [9].

* Corresponding author.
E-mail address: b.turan@fz-juelich.de (B. Turan).

http://dx.doi.org/10.1016/j.solmat.2014.02.029
0927-0248

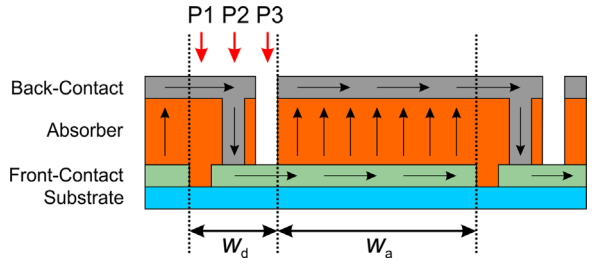

Fig. 1. Integrated series connection in p-i-n superstrate topology. The interconnection is realized by the three processes P1–P3. The relative area required for this is defined by the dead area width w_d and the width w_a of the remaining active part. The arrows indicate the current flow within the solar cell.

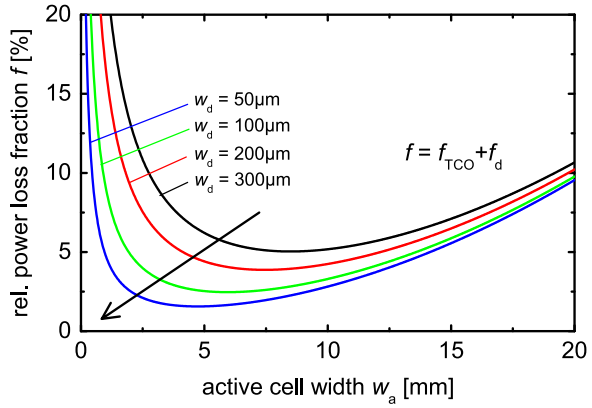

Fig. 2. Calculated sum f of fractional dead area losses f_d and current collection losses f_{TCO} vs. active cell stripe width w_a for an a–Si : H/µc–Si : H tandem silicon solar cell on ZnO:Al TCO parameterized over the interconnection width w_d (U_{mpp} = 1.11 V, J_{mpp} = 9.7 mA cm^{-2}, $R_{\square,TCO}$ = 8 Ω. Equations in Ref. [3]). The arrow indicates the direction of decreasing interconnection width w_d.

This work reports on the front-contact separation process P1 and the impact of the scribe width reduction on the electrical properties of the TCO front-contact material near the scribe edge after laser processing. Here, aluminum-doped zinc oxide (ZnO:Al) and fluorine-doped tin dioxide (SnO_2:F) TCO material on glass substrates were used and processing was done through the substrate side. All processing was done by nanosecond laser ablation with the wavelengths λ of 355 nm, 532 nm, and 1064 nm. The possible scribe width minimum was investigated with respect to a sufficiently high process stability. After processing, electrical properties of the TCO material near the scribe edge were investigated with conductivity Atomic Force Microscopy for scribe lines with a reduced width. To determine direct impact of laser processing on the solar cell Laser Beam Induced Current measurements were conducted as well. Furthermore, for the investigation of the surface morphology Scanning Electron Microscopy was used. All experiments and characterizations were done with and without subsequent wet-chemical surface treatment to differentiate between surface effects and changes within the whole TCO layer.

It will be shown that electrical properties and solar cell performance can be affected near the P1 scribe edge. These effects are most likely due to a massive redeposition of ablated material on the TCO surface rather than changes of the whole layer from heat-affected zone (HAZ) formation. This is also confirmed by the fact that with proper wet-chemical post-treatment, there is no significant influence on the active cell from laser processing within a broad range of laser parameters and processing wavelengths. For P1 processing scribe widths down to 10 µm are possible with a sufficiently high process stability and cell stripe insulation capability which is a significant reduction compared to the state-of-the-art of about 40 µm.

2. Experimental

2.1. Sample preparations

All experiments were performed on a commercial laser patterning system with *XYZ* translational stages. The axes are capable of feed-rates v up to 1000 mm s^{-1} in the *X*–*Y* directions and minimal step-sizes of 1 µm in the *Z* direction. The laser beam is directed onto the sample with fixed doublet and triplet lens systems through the glass side. A particle air suction system removes coarse debris of ablated material.

Diode-pumped Nd:YVO_4 solid-state nanosecond laser sources with the wavelengths λ of 355 nm, 532 nm, and 1064 nm are integrated into the scribing system. The output of the lasers exhibits a Gaussian intensity distribution. The measured pulse durations τ were between 7 ns and 40 ns (FWHM). The maximum average power P_{avg} of each laser source was determined with a thermopile sensor. These were 8 W (1064 nm), 3 W (532 nm), and 1 W (355 nm). Focal lengths f of 108.3 mm and 48 mm were used for 355 nm processing. For the wavelengths λ=532 nm and 1064 nm triplet lens systems with f=300 mm and 56 mm were chosen. The beam geometry in focus was measured with a laser beam profiler from PRIMES™. Table 1 shows the laser beam spot radii ω_0 in focus with stronger focusing optics.

Samples with 700 nm in-house sputtered ZnO:Al TCO material (1% $ZnOAl_2O_3$ sputter target, $R_{\square,TCO}$ = 4 Ω) [10] on 1.1 mm thick Corning™ Inc. glass and 900 nm SnO_2:F (type ANS14 ME from Asahi Glass Company, $R_{\square,TCO}$ = 8 Ω) TCO material [11] on 3 mm thick float glass substrates were processed.

Both material systems are characterized with and without subsequent wet-chemical cleaning or etching treatment after laser processing. For optimal light in-coupling and light trapping a rather rough surface texture between front-contact and absorber is required. Sputtered ZnO:Al TCO material exhibits a flat surface after deposition. It is usually etched for 30–40 s in 0.5% HCl solution to create the desired texture [10]. Here, to distinguish between surface dominated effects and changes within the whole layer, P1 experiments on ZnO:Al TCO were done with only 10 s etching. Profile measurements of the topography revealed that this short etching step decreases the initial thickness of 700 nm only by approx. 100 nm. However, optical properties can already be modified by the developing texture [12]. Fluorine-doped tin dioxide (SnO_2:F) TCO material created by Chemical Vapor Deposition (CVD) exhibits a rough surface texture so that no etching is required. Therefore, SnO_2:F was treated with the commercial cleaning agent DeContam™ in solution with deionized water. The substrate is then treated in an ultrasonic bath for 3 h at 60–70 °C before it is dried with nitrogen. This leads to no changes of the optical properties.

2.2. Characterization methods

The visible quality of the processing is inspected with optical microscopy. A Keithley 2600 series sourcing meter was used to

Table 1
Processing laser beam spot radius ω_0 in focus from beam profiler measurement for several focusing optics. Radius ω_0 is defined where the Gaussian peak intensity drops by 86% ($1/e^2$).

Focal length, f (mm)	Laser wavelength, λ (nm)	Spot radius, ω_0 (µm)
108.3	355	19.5
48	355	8.5
300	532	59.5
56	532	10.5
300	1064	44.6
56	1064	8.2